Appendix A

High Mass End of the Mass Function: The Star Formation History and Mass Function of h and χ Persei[1]

As discussed in chapter 6, our somewhat limited understanding of the intermediate mass stellar IMF is greatly overshadowed by our relative non-existent understanding of the lowest mass stellar and substellar end of the mass function. Almost as problematic is the high mass end of the IMF. Garnering a full census of high mass stars is difficult, due to the fact that they form, evolve, and die within just a few to tens of megayears, often before their lower mass counterparts have even reached the main sequence. Thus, deriving a field star IMF that extends to tens of solar masses is meaningless as the included high mass stars will necessarily be gigayears younger than the local intermediate and low mass field star population. A less biased view of the high mass IMF can be derived by examining a young, high mass cluster for which the highest mass stars have not yet evolved into supergiants. In this appendix I illustrate analysis of how an HR diagram can be used to assess the age and mass distributions of high mass clusters by describing a study I completed of the massive double cluster h & χ Persei. This work was carried out very early during my time at Caltech, prior to my work with the Quest-2 surveys of Taurus and USco and prior to

[1]A modified version of this appendix has been published previously as Slesnick, Hillenbrand, & Massey 2002, ApJ, 576, 880, and all work was done in collaboration with Phil Massey and Lynne Hillenbrand.

my work in the ONC. In this appendix, I summarize the results of this work only. A full analysis is given in Slesnick et al. (2002).

A.1 Motivation

The "double cluster" h and χ Persei (hereafter h/χ Per; also known as NGC 869 and NGC 884, respectively) is among the brightest, densest, and closest of the open clusters containing moderately massive stars. The double cluster has been studied extensively over the last century (e.g., Oosterhoff 1937, Bidelman 1943, Wildey 1964, Schild 1965, Crawford et al. 1970, Vogt 1971, Tapia et al. 1984, Waelkens et al. 1990) with resulting mean reddenings of $E(B-V) = 0.5$-0.6, and distance moduli in the range 11.4-12.0 mag (1.9-2.5 kpc). The clusters contain several tens of Be stars (e.g., Slettebak 1968, Bidelman 1947; see also Keller et al. 2001). Wildey's (1964) HR diagrams suggested several distinct episodes of star formation (7 Myr, 17 Myr, and 60 Myr), which would imply a spread of >50 Myr in the formation times of OB stars in a single (double) cluster! This age spread is larger than that claimed for any other well-studied open cluster, and was one of the primary motivations of my investigation in this region.

Most work prior to my study on h/χ Per has used photographic or single-channel photoelectric photometry with little emphasis on spectroscopy. Several very recent papers have used CCDs but consisted of photometric analysis only ($UBVI$/Hα, Keller et al. 2001; $ubvy/\beta$, Marco & Bernabeu 2001). Distance moduli in the range 11.6-11.8 mag and ages of 10-20 Myr have been found, with Marco & Bernabeu (2001) arguing (like Wildey 1964) for three distinct episodes of star formation, while Keller et al. (2001) find instead a single age. There is significant disagreement between various authors as to whether the reddenings, distances, and ages of the two clusters are identical or substantially (30%-50%) different. It is especially important to understand in detail the star formation history of h/χ Per as these clusters are widely used from professional review papers to basic introductory astronomy textbooks to illustrate stellar evolution at the high mass end of the main sequence. My main goals in this

study were to re-determine the age, and age spread in the double clusters, and to explore for the first time the mass function and the evidence for mass segregation.

My modern study of h/χ Per consisted of wide-field CCD *UBV* photometry for 4528 stars obtained from observations with the 0.9-m telescope at Kitt Peak National Observatory using the Mosaic CCD camera. Several hundred spectral types complement the photometric database. For hot stars, spectral data are needed to obtain accurate effective temperatures and consequently accurate extinction estimates and bolometric corrections (Massey 1998b, Massey 1998a) all necessary for locating a star in the HR diagram. Stars were selected for spectroscopy based on their brightness and colors, and blue optical spectroscopy was taken for 196 of the stars presumed to be the most massive (i.e., the brightest blue and red stars). The most luminous stars identified in the vicinity of h/χ Per are M, A, and B supergiants.

A.2 HR Diagram for h/χ Per

Figure A.1 is the HR diagram resulting from this study. Post-zero-age main sequence evolutionary tracks and isochrones are transformed from the log $T_{\rm eff}$ and M_{bol} values calculated by Schaller et al. (1992). All stars with MK spectral classifications of luminosity class I or III, and stars earlier than B5 with luminosity class IV or V were placed spectroscopically (larger, filled circles) while most other stars were placed photometrically (open circles). It is expected that stars near the cluster cores predominantly will be members, while stars further afield will be a mixture of both members and nonmembers. I constructed a contour plot of the spatial distribution of stars within the imaging field, and found that the stellar densities were enhanced by 2σ at identical radii of 7 arcminutes from each of the cluster cores. Thus, I use this radial criterion when describing stars near the nuclei. I also determined accurate centers for the two cores (α_{2000}=2:19:22.2, δ_{2000}=+57:09:00 for h Per, and α_{2000}=2:22:12.0, δ_{2000}=+57:07:12 for χ Per) by examining mass and number density contours. The left panel shows data for the entire imaging area while the right panel contains only stars within 7 arcmin of the cluster nuclei. No corrections for field star contamination

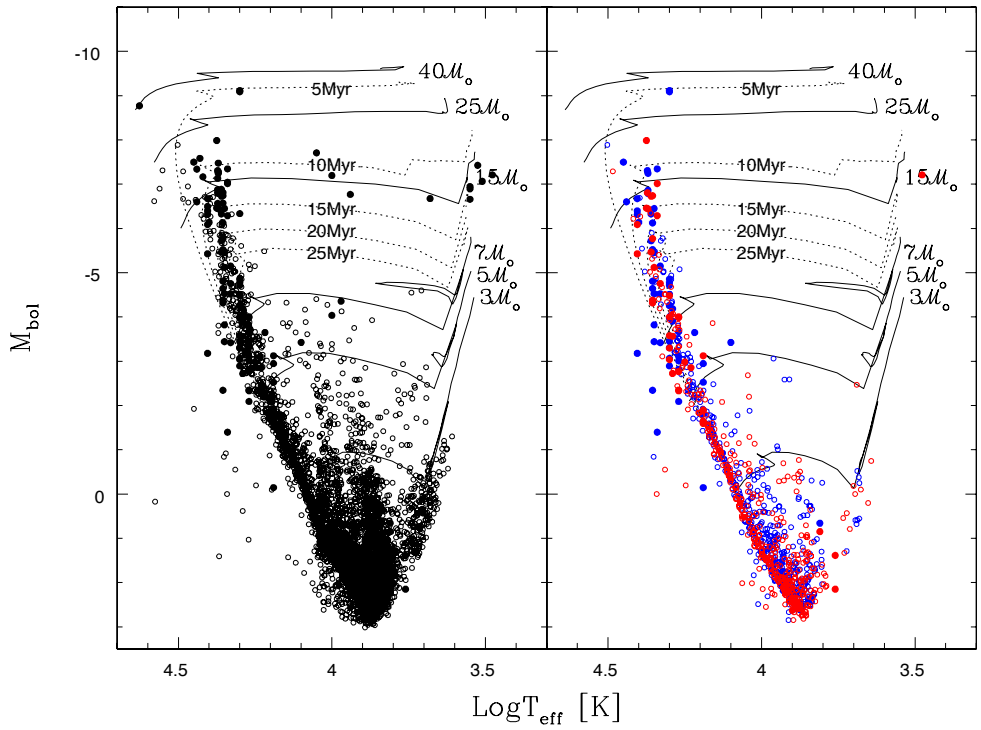

Figure A.1 The HR diagrams of h/χ Per are shown. On the left is shown all of the data: filled circles represent stars placed by means of spectroscopy and open circles represent stars for which only photometric data are available. On the right is shown only the stars within a 7 arcminute radius of the center of h (blue dots) and χ (red dots).

have been applied and the HR diagrams for the central regions of the clusters contain significantly less field star contamination, especially above the main sequence.

From these HR diagrams it is immediately seen that the high mass stars in the h/χ Per clusters are slightly evolved from the zero-age main sequence and that the most massive stars are only $\sim$20 to 30 $\mathcal{M}_\odot$. The data extend down to about $3\mathcal{M}_\odot$ before field star contamination becomes substantial.

A.3 Stellar Ages and the Age Distribution within h/χ Per

The dereddened CMD (figure A.2) is used to determine cluster ages. Data are shown in figure A.2 with a grid of isochrones computed at intervals of 0.1 Myr from 5 to 30 Myr.[2] Age determination is restricted to only the most luminous stars ($M_V < -3$) where the isochrones are substantially far apart to yield meaningful results. Obvious foreground contaminants were filtered out, e.g., $(B-V)_o > -0.2$ for $-3 > M_V > -5$. Red supergiants (RSGs) cannot be used for our age determinations, unfortunately, since the evolutionary tracks do not actually extend that far to the red. However, it is noted that the location of the RSGs in the CMD are consistent with the ages derived if the isochrones are extrapolated. For each of the clusters an essentially identical age was found: 12.8 Myr and 12.9 Myr for h and χ respectively. The formal errors of the mean on these determinations are 1 Myr, and the scatter is <0.01 mag level.

I do not find evidence for multiple distinct episodes of star formation despite the remarkable similarities between the dereddened CMD presented here and that of Wildey (1964). This difference in interpretation likely occurs because Wildey in his original analysis did not consider the possibility of field star contamination from G and

[2]The CMD was used rather than the HRD to determine ages in order to avoid the quantization problem introduced by spectral types. The ages of hot stars are very sensitive to $\log T_{\rm eff}$ (or $(B-V)_o$), and thus this quantization would introduce a spurious age spread. The spectral types *have* been employed in the CMD in order to derive $E(B-V)$. In a subsequent section the HRD is used to derive the mass function. The masses are primarily sensitive to an accurate determination of $M_{\rm bol}$, which is expected to be better determined using the bolometric corrections determined from spectral types.

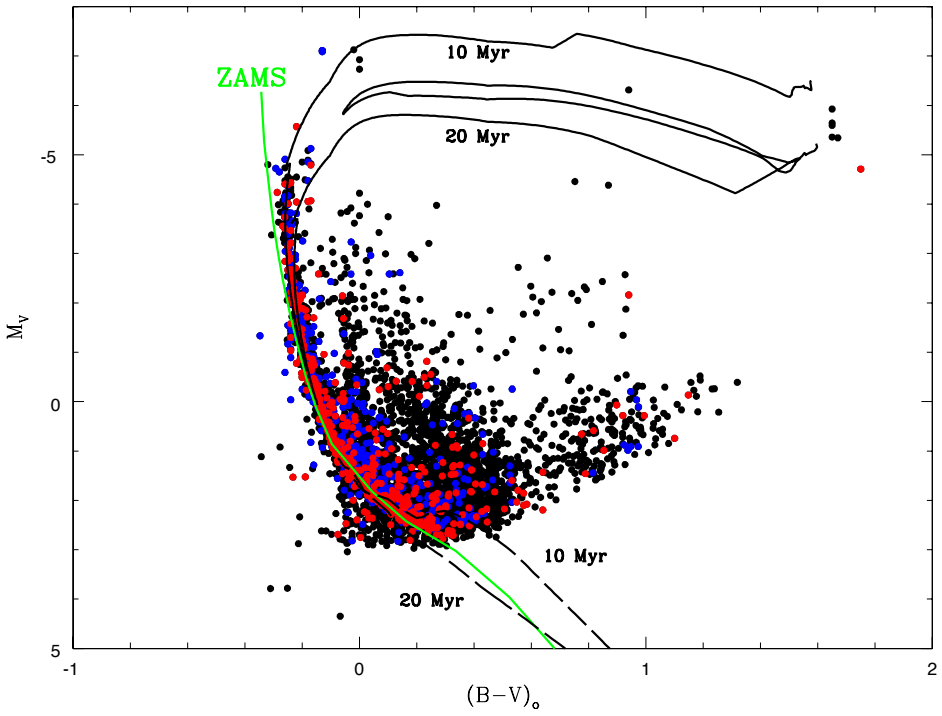

Figure A.2 The dereddened CMD for stars within 7 arcminutes of the center of h (blue) and χ (red) Per are shown now with the ZAMS and post-main-sequence isochrones of 10 and 20 Myr indicated. Corresponding 10 and 20 Myr pre-main-sequence isochrones are shown as dashed lines. The black points represent the rest of the stars in the full $0.98^\circ \times 0.98^\circ$ field.

K giants seen to large distances through the Galaxy. It is clear from the right panel of figure A.1 that when just the cluster nuclei are considered any apparent branching in the HR diagram is significantly diminished. There do exist several high-mass stars with uncharacteristically young ages as compared to the rest of the cluster. However, in most cases these stars are either not in the central regions of the clusters or their spectroscopically derived distance is inconsistent with their being cluster members.

A.4 Mass Function and Mass Segregation in h/χ Per

Masses are inferred for individual stars by interpolating between the mass tracks on the HR diagram. By counting the number of stars found in each mass bin, the "present day mass function" (PDMF) is derived. To the extent that star formation may be coeval, this is equivalent to the initial mass function (IMF) except for the depopulation of the highest mass bin.

In order to minimize the effect of field star contamination, PDMFs have been constructed only for the two regions within 7 arcmin of the cluster cores. In addition, a few stars found red-ward of the main-sequence, and presumed to be foreground contaminants, were excluded by eliminating stars in the region constrained between $M_{\rm bol} < -20.5 \times \log T_{\rm eff} + 82.5$ and $M_{\rm bol} > -5$. A lower mass cutoff of 4 $\mathcal{M}_{\odot}$ was used below which field and pre-main sequence star contamination dominate. At the high-mass end, it is expected that evolution through the supernova phase will have depleted stars above ∼15-20 $\mathcal{M}_{\odot}$, and so only the mass bins below this value have been used to compute the slope of the IMF. All of the higher-mass stars were combined into one mass bin. Following Scalo (1986), the quantity ξ is defined as the number of stars per mass bin divided by the difference in the base-ten logarithm of the upper and lower bin masses, and also by the surface area in kpc. The run of $\log \xi$ with log mass then provides the slope, Γ, of the IMF/PDMF. Values for the number of stars and for ξ are given in table A.1.

Table A.1. Mass function data for h/χ Per

Mass Range	h Per		χ Per	
$[\mathcal{M}_\odot]$	N	log ξ	N	log ξ
4.0-5.0	45	6.80	37	6.71
5.0-6.3	33	6.66	23	6.50
6.3-7.9	28	6.59	26	6.56
7.9-10.0	25	6.54	13	6.26
10.0-12.6	11	6.18	9	6.10
12.6-15.8	10	6.14	10	6.14
15.8-40.0	7	5.39	2	4.84

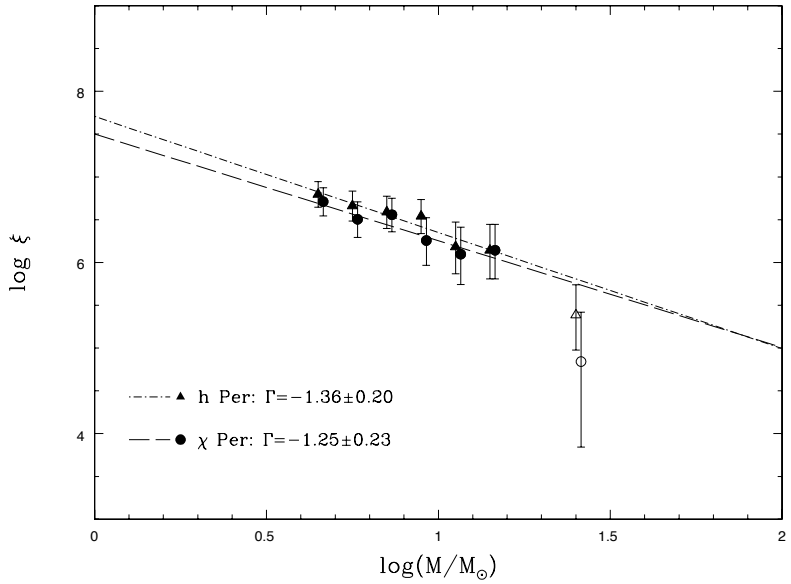

Figure A.3 The mass function is shown for the two clusters. Open symbols indicate an incomplete bin.

Figure A.3 shows PDMFs in the 4-16 $\mathcal{M}_\odot$ range for stars within 7 arcmin of the cluster centers. Error bars are based on $\pm\sqrt{N}$ statistics. Values are obtained of $\Gamma = -1.36 \pm 0.20$ for h Per and $\Gamma = -1.25 \pm 0.23$ for χ Per. Within the errors of the fits, both slopes are in good agreement with each other and also with the Salpeter value of $\Gamma = -1.35$. This result can be compared with what is known of the IMF in other young OB associations and clusters, where a weighted average yields $\Gamma = -1.1 \pm 0.1$ for the Milky Way and $\Gamma = -1.3 \pm 0.1$ for the LMC/SMC (Massey, 1998b) for similar mass stars. Thus, an IMF slope of $\Gamma = -1.3 \pm 0.2$ for h and χ is in no way unusual.

Based on extrapolation of the measured PDMFs to 120 $\mathcal{M}_\odot$, I estimate that $\sim$40 supernovae have occurred in the past in the central regions of the h/χ Per clusters. From this information, and assuming a constant mass function from 1 to 120 $\mathcal{M}_\odot$, I estimate the total stellar mass within each of the cluster centers down to 1 $\mathcal{M}_\odot$ to be 3700 $\mathcal{M}_\odot$ and 2800 $\mathcal{M}_\odot$ for h Per and χ Per , respectively. This is about 8-10 times that of the mass in >1 $\mathcal{M}_\odot$ stars in the younger Orion Nebula cluster ($\sim$450 $\mathcal{M}_\odot$) or the older Pleiades ($\sim 320\mathcal{M}_\odot$). For comparison, a "supercluster" like R136 in the LMC has a mass of roughly 3–4$\times 10^4 \mathcal{M}_\odot$ in >1 $\mathcal{M}_\odot$ stars (Hunter et al., 1996), about a factor of 10 greater than either h or χ and a factor of almost 100 greater than Orion or the Pleiades.

Figure A.4 explores the evidence for concentration and mass segregation in the two clusters. Only those stars satisfying the criteria for inclusion in the PDMF are considered in this figure. The top and middle panels of figure A.4 show that inside of 7 arcmin (i.e., the 2σ surface density contour), both the mass surface density and the number surface density begin to rise noticeably above the field star surface density, and then steepen considerably at $\sim$3 arcmin. The increase in density at smaller cluster radii is evidence of higher central concentration.

The histograms of the total mass/pc^2 as a function of radial distance (top panels of figure A.4) show that h Per is about twice as dense at its core compared to χ Per. This occurs both because h Per has $\sim$25% more stars at its center (as can be seen in the middle panels of figure A.4) and because it contains several high mass (>30

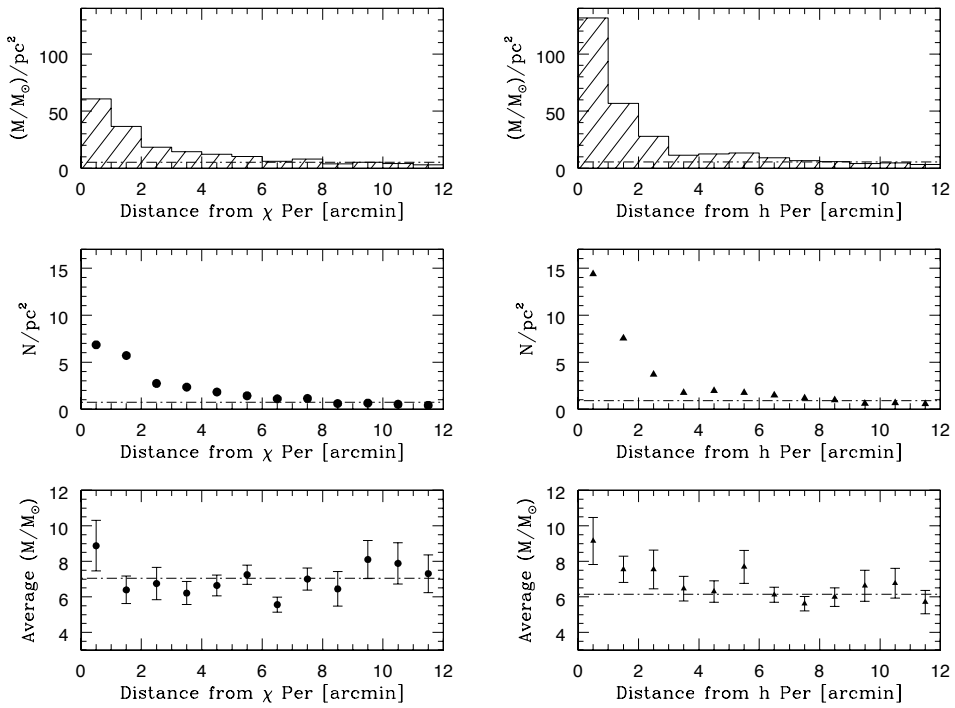

Figure A.4 The total mass per unit area (top panels), the number of stars per unit area (middle panels), and the average stellar mass per unit area (bottom panels) are shown as a function of radial distance for h Per (left) and χ Per (right). The data have been binned in 1 arcmin rings from the respective cluster centers. Horizontal dashed lines indicate the average of the values from 6 to 12 arcmin. Within the 2σ surface density enhancements (r = 7 arcmin), there is clear evidence in both h and χ Per for central concentration within 3 arcmin (top and middle panels), and also some evidence for mass segregation within 1-2 arcmin (bottom panels).

$\mathcal{M}_{\odot}$) B supergiants. However, the density profile of h Per falls off more rapidly than that of χ Per and the two clusters are roughly equivalent in mass density at a radius of $\sim$3 arcmin.

The bottom panels of figure A.4 show the average mass as a function of radial distance from the cluster centers. For h Per, we find a significant gradient inside of $\sim$7 arcmin in the mean mass vs. radial distance, suggestive of mass segregation. The data for χ Per is less convincing, yet we still find the mean stellar mass to be higher by $\sim$1.5–2σ within the central 1 arcmin. This phenomenon has been claimed with varying degrees of strength in other open clusters in the Galaxy (e.g., the Orion Nebula Cluster; Hillenbrand & Hartmann 1998 and references therein) and in the Magellenic Clouds (e.g., R136; Hunter et al. (1995), and NGC 1805 and NGC 1818; de Grijs et al. 2002). However, unlike their younger counterparts, the mean mass gradient in h/χ Per may not be primordial, i.e., associated with the formation of the clusters. Assuming a velocity dispersion of σ_v $\approx$3 km/s and a 7 arcmin (4.79 pc) cluster radius, each of the cluster nuclei has a crossing time of $\sim$1.56 Myr. Given that the clusters are $\sim$13 Myr old, the age/t_{cross} $\approx$8 and hence dynamical relaxation may indeed play some part in the observed mass segregation.

A.5 Summary of the h/χ Per Survey

I have studied the h and χ "double cluster" using modern imaging and spectroscopic techniques. My conclusions differ with those of previous studies such as Wildey's (1964) largely due to my recognition of the significant effect that field star contamination has on the determination of cluster ages. Inclusion of foreground younger stars and GK giants can easily lead to apparent branching in the HR diagram which has been misinterpreted in the past as an age spread. I find mean ages of 12.8 Myr for each of the two clusters and no evidence for multiple epochs of star formation.

The present day mass function yields a slope consistent with that found in other well-studied Galactic OB associations and clusters ($\Gamma \sim -1.1 \pm 0.1$, see Massey (1998b)), and is essentially Salpeter ($\Gamma = -1.35$). In addition, I do find some evidence

of mass segregation. The total masses are 3700 $\mathcal{M}_{\odot}$ for h Per and 2800 $\mathcal{M}_{\odot}$ for χ Per, for stars with $> 1\mathcal{M}_{\odot}$.